Synthesis and Characterization of *In Situ* Polymerized Segmented Thermoplastic Elastomeric Polyurethane/ Layered Silicate Clay Nanocomposites

Mi Young Choi,[1] S. Anandhan,[1] Ji Ho Youk,[1] Du Hyun Baik,[2] Seung Won Seo,[3] Han Sup Lee[1]

[1]*Department of Textile Engineering, Inha University, Incheon 402 751, Korea*
[2]*Department of Textile Engineering, Chungnam National University, Daejeon 305-764, Korea*
[3]*R&D Center for Fibers and Textiles, Hyosung Co, Anyang 431-080, Korea*

Received 2 May 2005; accepted 16 April 2006
DOI 10.1002/app.24734
Published online in Wiley InterScience (www.interscience.wiley.com).

ABSTRACT: Nanocomposites based on thermoplastic elastomeric polyurethane (TPU) and layered silicate clay were prepared by *in situ* synthesis. The properties of nanocomposites of TPU with unmodified clay were compared with that of organically modified clay. The nanocomposites of the TPU and organomodified clay showed better dispersion and exhibited superior properties. Exfoliation of the clay layers was observed at low organoclay contents, whereas an intercalated morphology was observed at higher clay contents. As one of major purposes of this study, the effect of the silicate layers in the nanocomposites on the order–disorder transition temperature (T_{ODT}) of the TPU was evaluated from the intensity change of the hydrogen-bonded and free carbonyl stretching peaks and from the peak position change of the N—H bending peak. The presence of the organoclay increased T_{ODT} by approximately 10°C, which indicated improved stability in the phase-separated domain structure. The layered silicate clay caused a tremendous improvement in the stiffness of the TPU; meanwhile, a reduction in the ultimate elongation was observed. © 2006 Wiley Periodicals, Inc. J Appl Polym Sci 102: 3048–3055, 2006

Key words: elastomers; nanocomposites; synthesis; thermoplastics; transitions

INTRODUCTION

Polyurethane (PU) is a polymer having a segmented microstructure and possessing excellent biocompatible, elastic, and abrasive properties.[1] The morphology of PU determines its mechanical, thermal, and water absorption properties.[2–4] The hard segments are formed by the addition of a chain extender to the diisocyanate, and the soft segments consist of a long flexible polyether or polyester chain that interconnects two hard segments. At temperatures lower than the order–disorder transition temperature (T_{ODT}), the low-melting soft segments are incompatible with the polar and high-melting hard segments, which leads to a phase-separated microstructure.[5,6] The development of crystallinity in the hard segments can be a strong driving force for phase separation, and the crystallites melt when heated above the melting temperature, and a homogeneous melt is formed.

In recent times, polymer/layered silicate nanocomposites have drawn a great deal of attention because they often exhibit tremendous improvements in material properties compared to virgin polymers or conventional microcomposites or macrocomposites. These improvements include a high modulus, increased strength and thermal stability, decreased gas permeability and flammability, and increased biodegradability of biodegradable polymers.[7–14]

Montmorillonite (MMT)-based clays were used for the preparation of the nanocomposites in this study. MMT is a naturally occurring 2 : 1 phyllosilicate, which has the same layered and crystalline structure as talc and mica but a different layer charge.[15] The Na^+ or Ca^{2+} ions residing in the interlayers can be replaced by organic cations such as alkyl ammonium ions or phosphonium ions by an ion-exchange reaction to render the hydrophilic layered silicate organophilic so that polymer chains can be intercalated, which thus causes the clay layer to be either swollen or exfoliated.[16]

Because PU has been used in various applications, it is important to finely control the physical properties of it by controlling the chemical and physical structure. Therefore, PU/layered silicate clay nanocomposites are excellent candidates for the achievement of

Correspondence to: H. S. Lee (hslee@inha.ac.kr).
Contract grant sponsor: Basic Research Program of the Korea Science & Engineering Foundation; contract grant number: R01-2003-000-10215-0.
Contract grant sponsor: Ministry of Science and Technology (MOST), Korea (for Synchrotron X-ray experiments at Pohang Light Source (PLS).
Contract grant sponsor: Pohang Steel Company (POSCO), Korea (for Synchrotron X-ray experiments at Pohang Light Source (PLS).

enhanced physical properties without the alteration of the chemical structure of PU.[17] PU/MMT nanocomposites have been synthesized and characterized extensively ever since they were initially synthesized with MMT, in which Na^+ or Ca^{2+} ions residing initially in the interlayers were exchanged with alkyl ammonium ions to expand the silicate layer spacing.[18] The effects of silicate layers on the mechanical,[19–21] thermal,[22–24] and diffusional[25–27] properties of PU nanocomposites have been studied in many works. If expanded MMT is used in the PU nanocomposite, the breaking strength and modulus have been reported to be enhanced as much as 600[19] and 300%,[23] respectively, and resistance to the thermal degradation was significantly increased. Even though the thermal stability of PU nanocomposites have been extensively studied, most thermal analyses have been dedicated to the evaluation for the effect of the silicate layers in the nanocomposite on the thermal degradation.

Because PU is a thermoplastic elastomer, it forms a phase-separated domain structure at temperatures below T_{ODT} and turns into plastic melt as the temperature increases above T_{ODT}. Order–disorder transition behavior is one of the most important behaviors of PU. In general, the external shape of PU material is formed above T_{ODT}, and the PU products are used below T_{ODT} during use in any practical applications.[1] Even though the exact value of T_{ODT} is a very important parameter for many PU materials, study of the effect of silicate layers on the thermal stability of the domain structure and on T_{ODT} is far from complete.

In this study, thermoplastic elastomeric polyurethane (TPU)/MMT-based clay nanocomposites were prepared by an *in situ* intercalative polymerization method. The clay was swollen with the prepolymer; then, the chain extension was carried out so that the polymer chains could intercalate on the galleries of the clay. One of our main aims was to study the effect of nanocomposite formation on the order–disorder transformation of the TPU. The effects of MMT-based clay on the physical structure of TPU was also investigated along with the thermal and mechanical properties.

EXPERIMENTAL

Synthesis of TPU/clay nanocomposites

The details of the poly(tetramethylene glycol) (PTMG) and organically modified montmorillonite clay (O-MMT) used in this study are given in Table I. The hard segment of the TPU was formed from 4,4′-methylenebis (phenylisocyanate) (MDI) and 1,4-butanediol (BD). The soft segment was formed from PTMG. MDI and PTMG were dried in a vacuum oven before use, and BD was stored on 4-Å molecular sieves. Both unmodified MMT (Na-MMT) and O-MMT were used after heating at 130°C for 24 h to remove molecular water in the galleries. The TPU/clay nanocomposites were prepared by an *in situ* polymerization method, and the molar ratio of MDI/BD/PTMG was 4 : 3 : 1, and it was denoted as MBP431. The nanocomposites were synthesized by a two-step reaction.[28,29] In the first step, PTMG was reacted with an excess of MDI at 85°C for 2 h to form a prepolymer end-capped with isocyanate groups. In the second step, clay dispersed in freshly distilled dimethyl acetamide was added to the prepolymer at room temperature; then, the chain extender (BD) mixed with dibutyltindilaurate was added. The chain extension reaction was carried out at 85°C for 2 h. The reactions that occurred during the TPU/clay nanocomposite syntheses are shown in Scheme 1.

TABLE I
Details of the Materials

Material	Details
PTMG	Weight-average molecular weight = 1800 g/mol (Hyosung Co., Anyang, Korea)
Cloisite-30B	Cation exchange capacity = 90 mequiv/100 g; specific gravity = 1.98 g/cc (Southern Clay Products Gonzalez, TX)

Wide-angle X-ray diffraction (WAXD) studies

All samples of TPU and the nanocomposites were annealed at 80–100°C for 12 h in a vacuum oven to ensure optimum microphase separation and to enhance crystallinity. WAXD measurements were performed with a Rigaku diffractometer (Tokyo, Japan) with Ni-filtered Cu Kα radiation (λ = 0.154 nm), and a Synchrotron X-ray setup at the 4C1 Beamline at the Pohang Accelerator Laboratory, Korea, was also used for enhanced sensitivity for some selected samples.[30]

Transmission electron microscopy (TEM)

TEM studies of the representative samples were carried out with a Philips transmission electron microscope (Tokyo, Japan) at an accelerating voltage of 120 kV. We prepared the samples, about 50 nm thick, by cryomicrotoming in an RMC ultracryomicrotome (Tokyo, Japan) with glass knives (made with an RMC knife maker) after freezing the specimens below their glass-transition temperature (at −90°C) with liquid nitrogen. The cryomicrotomed sections were deposited onto 400-mesh copper grids and were dried in a vacuum oven at 80°C before TEM analysis. The cryomicrotomed section of the pure TPU was stained with a 1% solution of RuO_4.

Fourier transform infrared studies

A Bruker IFS66V/S FTIR spectrometer (Ettingen, Germany) was used to study the order–disorder

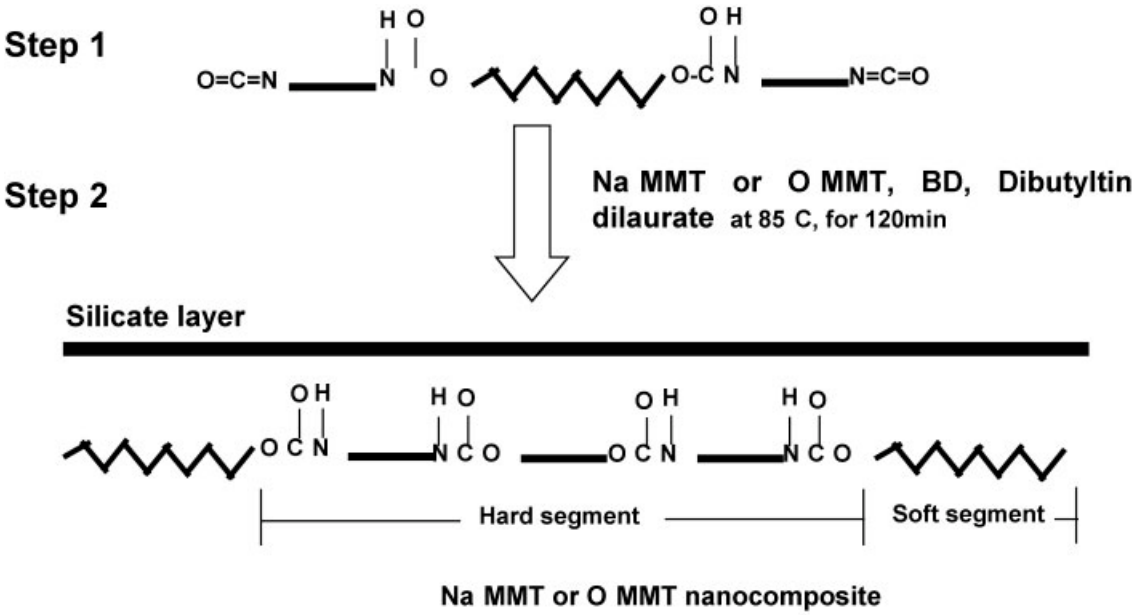

Scheme 1 Synthesis route for the TPU/layered silicate clay nanocomposites.

transitions of the nanocomposites and TPU. The samples were solvent-cast from their dimethyl acetamide solutions onto KBr discs and were dried in a vacuum oven and used for analysis. FTIR spectra were obtained with a resolution of 2 cm^{-1}, and 32 scans were averaged for each spectrum. To investigate the effect of clay on T_{ODT} of PU, the FTIR spectra were recorded at a temperature range of 40–220°C and a temperature interval of 10°C with the temperature-control device built in this laboratory.[31] All absorbance was obtained from the peak height from the local baseline.

Differential scanning calorimetry (DSC)

DSC thermograms were recorded in a Shimadzu TA-50 differential scanning calorimeter (Kyoto, Japan). The samples (~ 10 mg) sealed under aluminum pans were scanned from 25 to 250°C under a nitrogen blanket with a flow rate of 40 mL/min.

Mechanical properties

Mechanical properties were studied with an Instron (Hounsfield, H10K-S Surrey, UK) UTM according to ASTM D 638, and the samples were punched out with an ASTM D 638 type IV die. The testing was done at 25°C and at a crosshead speed of 10 mm/min.

RESULTS AND DISCUSSION

Morphology of the nanocomposites

The WAXD results of Na-MMT, O-MMT, the TPU/clay nanocomposites containing 1% Na-MMT and 1% O-MMT are shown in Figure 1. The O-MMT showed a (001) diffraction peak at 4.8°. The gallery spacing (d) values of Na-MMT and O-MMT were 12.58 and 18.54 Å, respectively. The gallery spacing in O-MMT was higher than that of Na-MMT because of the presence of the organic modifier (methyl tallow bis-2-hydroxyethyl quaternary ammonium ion). There were no peak maxima in the WAXD curves of the PU containing 1% Na-MMT and 1% O-MMT, which indicated that the major portion of the Na-MMT and O-MMT in the corresponding nanocomposites existed in an exfoliated state. The WAXD patterns of the TPU/Na-MMT nanocomposites containing various amounts of Na-MMT are shown in Figure 2. The nanocomposites containing 3 and 5% Na-MMT displayed broadened peaks in their respective WAXD patterns. The results in Figure 2 show that the clay had an appreciable

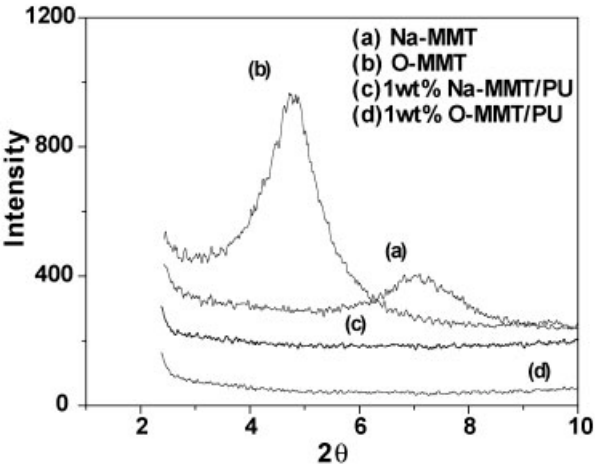

Figure 1 WAXD patterns of Na-MMT, O-MMT, 1 wt % Na-MMT/PU, and 1 wt % O-MMT/PU.

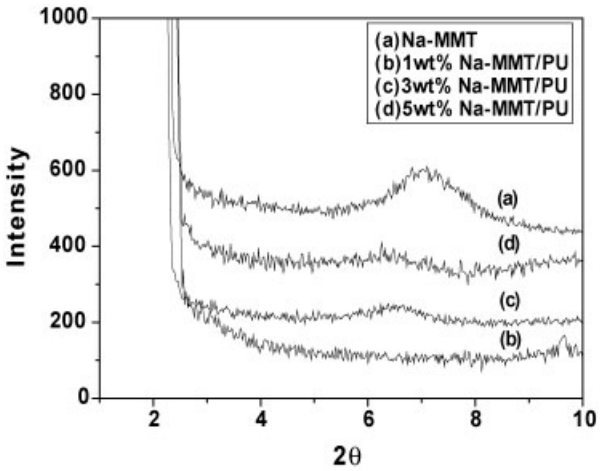

Figure 2 WAXD patterns of Na-MMT/PU nanocomposites obtained with the conventional X-ray source.

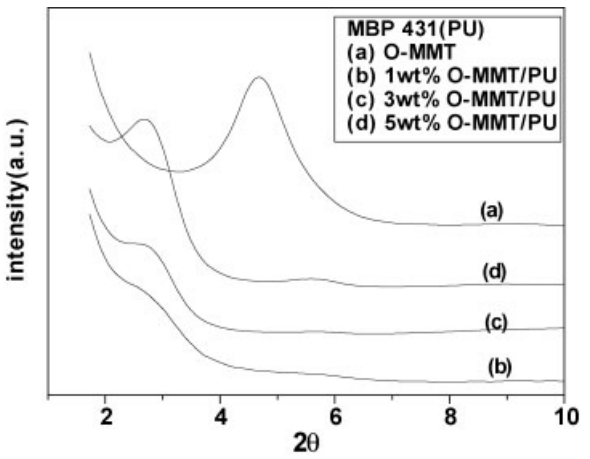

Figure 3 WAXD patterns of O-MMT/PU nanocomposites obtained with the Synchrotron X-ray source.

amount of intercalated structure. Furthermore, the expansion of the gallery spacing was minimal.

The WAXD patterns of nanocomposites containing various amount of O-MMT were also obtained with a conventional X-ray diffractometer (data not shown). The peak maxima of some of the O-MMT/PU samples were not obvious because of the low sensitivity of the conventional X-ray setup and also the small amount of the layered structure showing X-ray diffraction peaks. The peak maximum of pure O-MMT was observed at 4.8°, which was lower than the corresponding value of pure Na-MMT. The peak maxima of some of the samples appeared to be overlapped with the tail of the X-ray main beam. To unambiguously verify the existence of a small amount of the layered structure in O-MMT/PU samples, WAXD profiles were obtained from the Synchrotron X-ray facility at Pohang Accelerator Laboratory in Korea, and the results are shown in Figure 3.

As expected, the diffraction peaks for all of the samples could be verified. However, the diffraction peaks were shifted down to about 2.8°, which indicated the expansion of the basal spacing from 1.8 to 3.1 nm. Even for the 1 wt % O-MMT/PU sample, whose diffraction peak could not be verified clearly with the conventional setup (Fig. 1), the diffraction peak was clearly observed. A small portion of the layered silicates still existed as an expanded, intercalated state for this sample. For samples containing higher amounts of O-MMT, however, diffraction peaks were much more obvious, which indicated the unambiguous existence of the intercalated structure of long basal spacing.

The TEM photomicrographs revealed poor dispersion of the Na-MMT in the TPU matrix, and moreover, some tactoids were also seen (Fig. 4). The nanocomposite containing 1% O-MMT had lot of exfoliated clay layers dispersed uniformly in the TPU matrix (Fig. 5); meanwhile, some nonexfoliated clay tactoids were also present (not shown here). The TPU/O-MMT nanocomposites containing 3 and 5% organoclay had intercalated morphologies. Some exfoliated clay layers were also seen in the TEM photomicrographs.

Effect of clay on the order–disorder transition of TPU

TPU is a segmented block copolymer having thermoplastic elastomeric characteristics. The hard segments (formed by MDI) form domains that are dispersed in a continuous matrix of the soft, rubbery segments formed by PTMG segments. The size of the domains is in the range 2–4 nm as shown by high-resolution TEM photomicrographs of RuO_4-stained TPU (data not shown here).

One of our main objectives in the development of the silicate clay-based nanocomposites was to enhance T_{ODT} of TPU. Because the hard domains disappeared

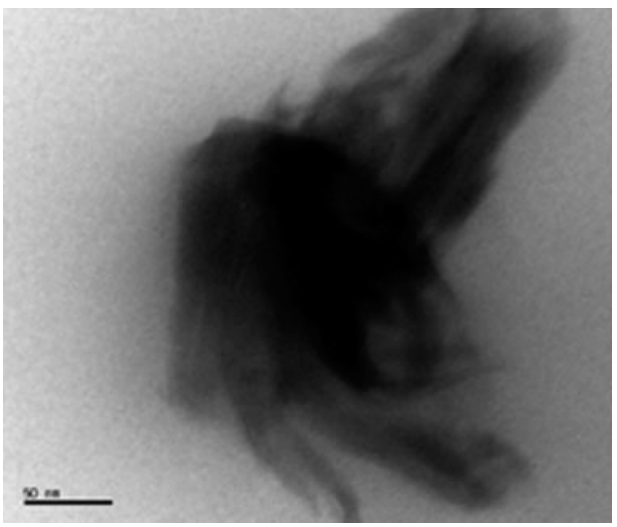

Figure 4 TEM photomicrograph of the 3 wt % Na-MMT/PU nanocomposite (scale bar = 50 nm).

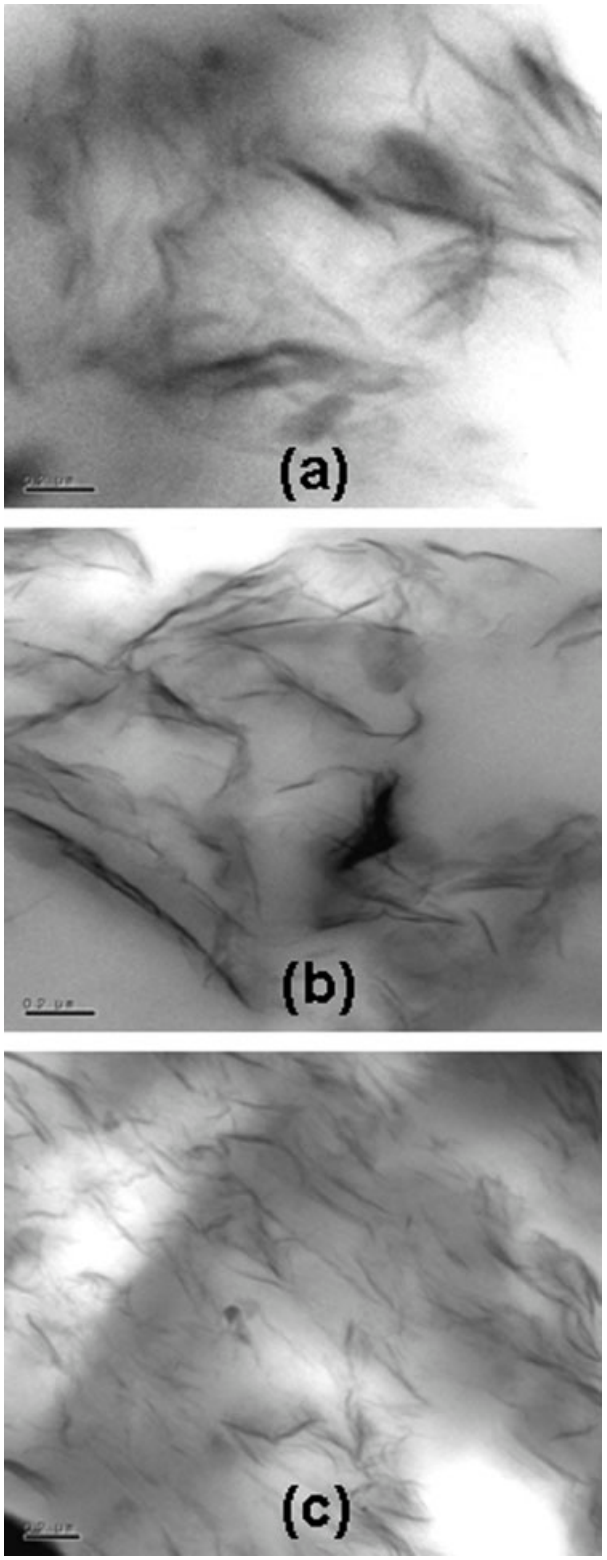

Figure 5 TEM photomicrographs of the O-MMT/PU nanocomposites containing (a) 1, (b) 3, and (c) 5% O-MMT (scale bar = 200 nm).

due to the dissolution of the hard domains in the soft matrix above T_{ODT}, it was important to maintain the phase-separated structure during various TPU processing operations. On transformation from the homogeneous state to the phase-separated state, most hard segments aggregate and form hard domains in the soft matrix. Typically, PU is extensively hydrogen-bonded, with the donor being the NH group of the urethane linkage and the acceptor being the carbonyl group of the urethane linkage of the neighboring polymer chains. Because the hard segments contain urethane groups, they can form hydrogen bonds with other hard segments inside the hard domain, and the formation of hydrogen bonding can be a strong driving force for phase separation. Therefore, one can monitor the extent of phase separation by following the change in the degree of hydrogen bonding. The order–disorder transition, sometimes called the *microphase separation transition*, of the TPU and its nanocomposites with O-MMT were studied by FTIR and DSC methods.

Figures 6 and 7 show the C=O stretching peak region in the FTIR spectra of MBP431 and MBP431/

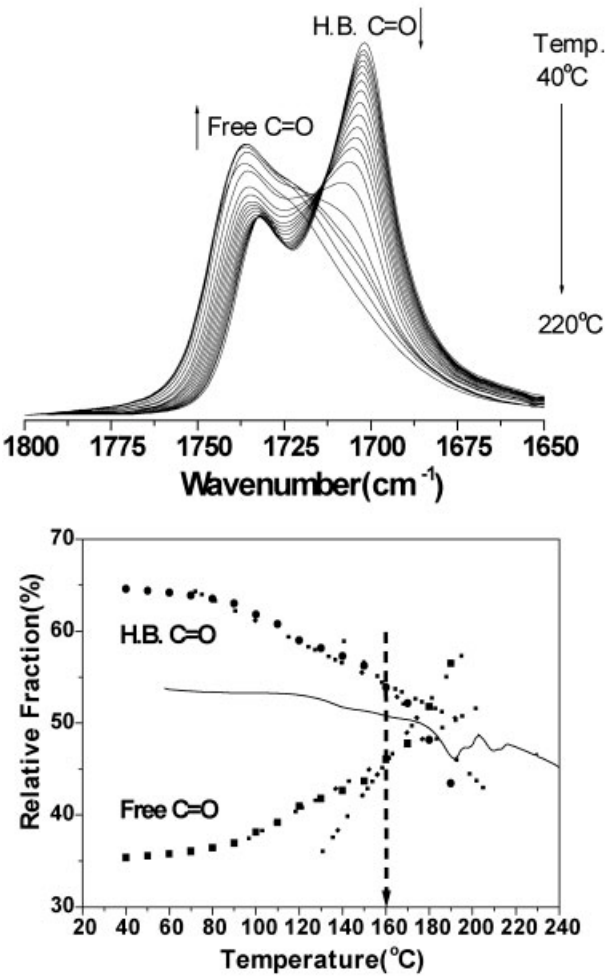

Figure 6 (Top) FTIR spectra of the C=O stretching peak of the pure TPU at various temperatures (Temp.'s). (Bottom) The relative fractions of two carbonyl peaks plotted as a function of temperature along with the DSC thermogram (solid line).

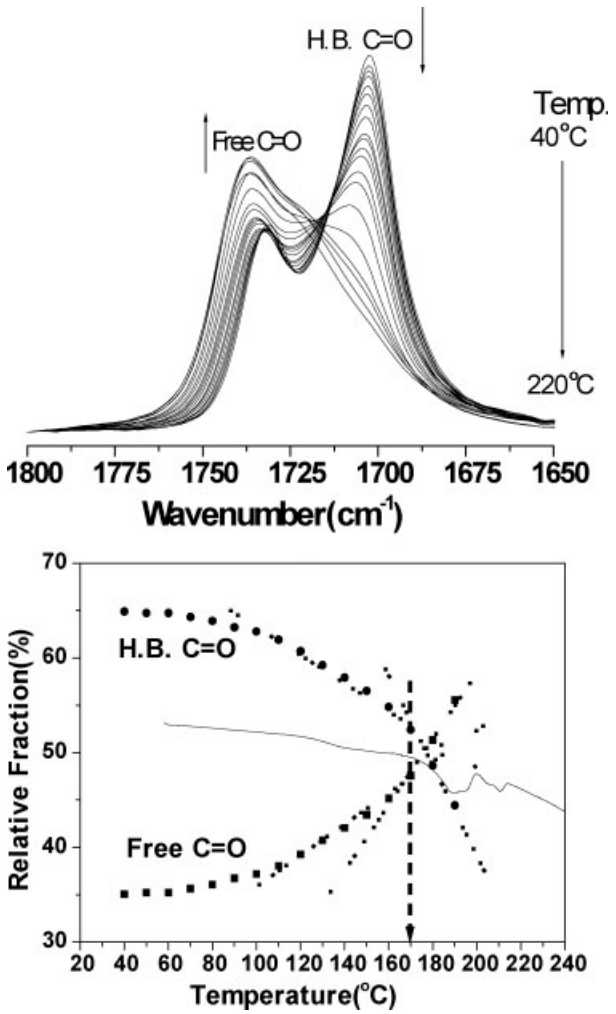

Figure 7 (Top) FTIR spectra of the C=O stretching peak of the 1 wt % O-MMT/PU nanocomposite at various temperatures (Temp.'s). (Bottom) The relative fractions of two carbonyl peaks plotted as a function of temperature along with the DSC thermogram (solid line).

1 wt % O-MMT nanocomposites, respectively, as a function of temperature. At low temperature, the wave number of the C=O stretching peak of the free urethane group (Free C=O) was about 1737 cm^{-1} and that of the hydrogen-bonded urethane group (H.B.C=O) was about 1700 cm^{-1}; the intensity of the hydrogen-bonded carbonyl group was higher than that of the free urethane carbonyl group. As the temperature increased, the intensity of the free C=O group peak increased, whereas that of the hydrogen-bonded C=O group decreased. The relative fraction of both carbonyl peaks are also shown at the bottom of each figure.

As shown in Figures 6 and 7, the intensity of both the free and hydrogen-bonded C=O peaks of MBP431 started to change as temperature increased above 80°C, which was close to the annealing temperature. These gradual changes appeared to be associated with the order–disorder transition behavior of a small amount of short-range order hard domains, which was not clearly observed in the DSC thermogram also given in the corresponding figures for comparison. As the temperature increased further, the slopes changed gradually up to about 200°C. Even though it was difficult to pinpoint the starting temperature of the major transitions, the order–disorder transition of the long-range order hard domain appeared to start at about 160°C for pure TPU (Fig. 6), and the corresponding value for the TPU/1 wt % O-MMT nanocomposite was about 170°C (Fig. 7). This seemed to indicate that the stability of the hard domains of the TPU might have been improved by the incorporation of nanosize layers of the silicate clay. The DSC curves in Figures 6 and 7 show major endothermic peaks at approximately 190°C, which were attributed to the dissociation of long-range order hard domains. The transitions estimated from FTIR data were observed at temperatures somewhat lower than the corresponding ones from the DSC thermograms. Even though more studies might be carried out to further clarify that difference, it might be related to the fact that the DSC peak was related to the overall structural change, whereas the FTIR spectrum was

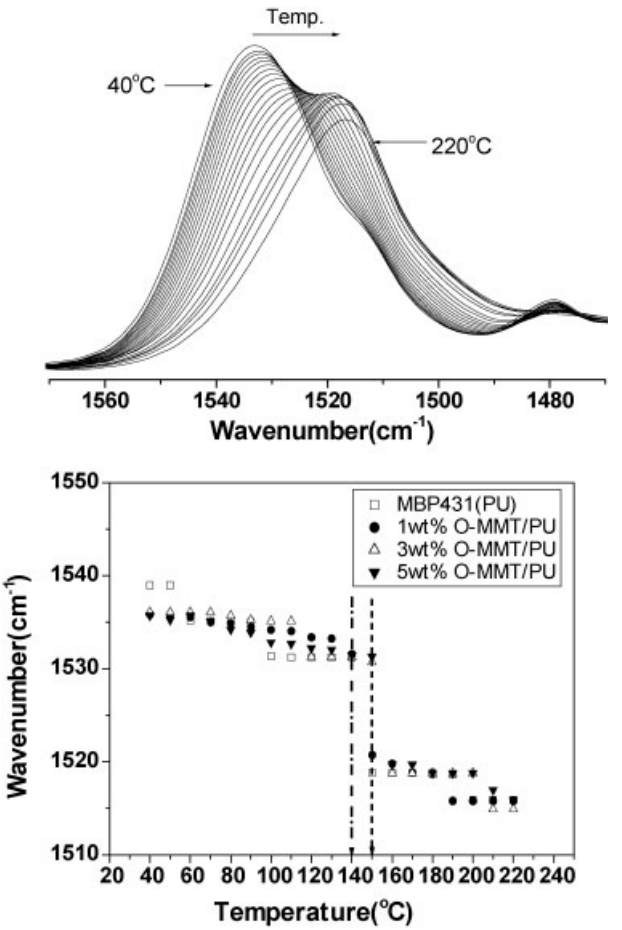

Figure 8 (Top) FTIR spectra of the N—H bending peak of the pure TPU at various temperatures (Temp.'s) along with (bottom) the plot of peak position as a function of temperature of the O-MMT/PU nanocomposites.

TABLE II
Mechanical Properties of the TPU/Clay Nanocomposites

Sample	Tensile strength (MPa)	Elongation at break (%)	Young's modulus (MPa)
MBP431(PU)	68.3	1420	24.1
1 wt % Na-MMT/PU	51.2	1180	24.4
3 wt % Na-MMT/PU	34.8	980	28.6
5 wt % Na-MMT/PU	37.1	998	49.1
1 wt % O-MMT/PU	28.6	990	26.2
3 wt % O-MMT/PU	27.9	660	46.3
5 wt % O-MMT/PU	31.0	575	53.3

sensitively affected by the change in local interchain interactions.

To further evaluate the effect of nanocomposite formation on the major transition temperature of TPU, the N—H bending peaks obtained during the heating process were analyzed. The top of Figure 8 shows the NH bending peak region in the FTIR spectra of pure TPU as a function of temperature. At low temperatures, the wave number of the NH bending peak was about 1534 cm^{-1}. As the temperature increased, the extent and average strength of hydrogen bonding decreased, which resulted in the decreased NH bending wave numbers. For MBP431 (shown in Fig. 8), the NH bending wave numbers decreased down to about 1517 cm^{-1} at 180°C. Also shown in Figure 8 is the plot of peak position against temperature for pure TPU and the TPU/O-MMT nanocomposites containing different amounts of O-MMT. Initially, the wave number started decreasing slowly as the temperature increased. However, there was an abrupt change at about 140°C for pure TPU and the TPU/1 wt % O-MMT nanocomposite presumably due to the order–disorder transitions. A corresponding change in nanocomposites containing higher amounts of O-MMT was observed at about 150°C. Even though the temperature range showing the sudden decrease of N—H bending peaks was not directly correlated with the corresponding temperature range showing the abrupt C=O stretching peak intensity shown in two previous figures, the silicate layers in the nanocomposite unambiguously enhanced the dissociation temperature of the hydrogen bonding between C=O and N—H groups. The thermal stability of the phase-separated domain structure that was sensitively affected by the extent and strength of the hydrogen bonding between hard segments should have been, therefore, also enhanced by the organoclay layers.

Mechanical properties

The mechanical properties of the pure TPU, TPU/Na-MMT nanocomposites, and TPU/O-MMT nanocomposites are displayed in Table II, and the stress–strain curves are shown in Figure 9. The tensile strength and ultimate elongation values decreased with the addition of Na-MMT or O-MMT. There was, however, a significant improvement in the Young's modulus values with increasing levels of both Na-MMT and O-MMT. The same trend was observed for TPU/layered silicate clay nanocomposites by Finnigan et al.[32] Interestingly, O-MMT caused a larger reduction in the tensile and elongation properties than Na-MMT. Meanwhile, the enhancement of Young's modulus caused by O-MMT was higher than that caused by Na-MMT. This appeared to be due to enhanced interaction between TPU and O-MMT.

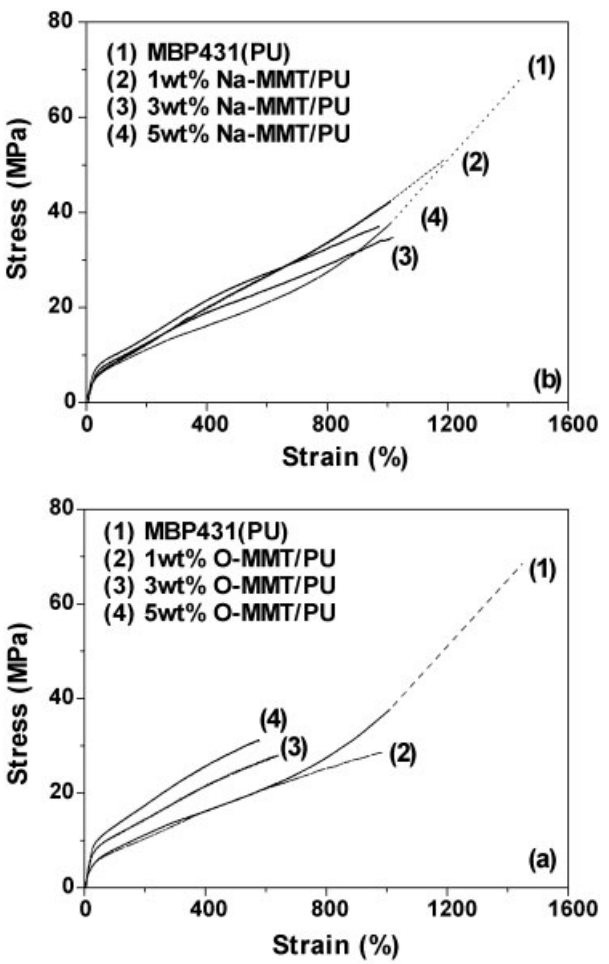

Figure 9 Tensile stress–strain curves of TPU nanocomposites containing (a) O-MMT and (b) Na-MMT.

CONCLUSIONS

Nanocomposites based on segmented TPU and silicate clay were prepared by *in situ* synthesis. The X-ray diffraction studies revealed that majority of organoclay in the TPU matrix was exfoliated at low organoclay contents, whereas the extent of intercalation was increased at higher clay contents. The effect of the silicate layers on T_{ODT} of the TPU was evaluated from the temperature dependence of peak intensities of the hydrogen-bonded and free carbonyl stretching peaks. The organoclay raised T_{ODT} as much as 10°, and this seemed to be due to the increased stability of the phase-separated structure because of the restriction caused by the clay layers for the mobility of the hard domains. The increased T_{ODT} was confirmed again from the temperature dependence of the N—H bending peak positions. The layered silicate clay caused a tremendous improvement in the stiffness of the TPU; meanwhile, it caused a reduction in the tensile strength and ultimate elongation.

References

1. Hepburn, C. Polyurethane Elastomers; Elsevier Applied Science: New York, 1991; p 51.
2. Garrett, J. T.; Runt, J.; Lin, J. S. Macromolecules 2000, 33, 6353.
3. Miller, J. A.; Lin, S. B.; Hwang, K. S.; Wu, K. S.; Gibson, P. E.; Cooper, S. L. Macromolecules 1985, 18, 32.
4. Wang, C. B.; Cooper, S. L. Macromolecules 1983, 16, 775.
5. Tien, Y. I.; Wei, K. H. Macromolecules 2001, 34, 9045.
6. Meckel, W.; Goyert, W.; Wieder, W. In Thermoplastic Elastomers—A Comprehensive Review; Holden, G.; Legge, H. R.; Quirk, R.; Schroeder, H. E., Eds.; Hanser: Munich, 1987; p 16.
7. Ray, S. S.; Okamato, M. Prog Polym Sci 2003, 28, 1539.
8. Le Baron, P. C.; Wang, Z.; Pinnavaia, T. J. Appl Clay Sci 1999, 15, 11.
9. Xu, R.; Manias, E.; Snyder, A. J.; Runt, J. Macromolecules 2001, 34, 337.
10. Bharadwaj, R. K. Macromolecules 2001, 34, 1989.
11. Messersmith, P. B.; Giannelis, E. P. J Polym Sci Part A: Polym Chem 1995, 33, 1047.
12. Gilman, J. W. Appl Clay Sci 1999, 15, 31.
13. Gilman, J. W.; Jackson, C. L.; Morgan, A. B.; Harris, R., Jr.; Manias, E.; Giannelis, E. P.; Wuthenow, M.; Hilton, D.; Phillips, S. H. Chem Mater 2000, 12, 1866.
14. Dabrowski, F.; Bourbigot, S.; Delbel, R.; Bras, M. L. Eur Polym J 2000, 36, 273.
15. Giese, R. F.; Van Oss, C. J. Colloid and Surface Properties of Clays and Related Minerals; Marcel Dekker: New York, 2002.
16. Ma, X.; Lu, H.; Liang, G.; Yan, H. J Appl Polym Sci 2004, 93, 608.
17. Lee, H. S.; Choi, M. Y.; Anandhan, S.; Baek, D. H.; Seo, S. W. Presented at the Polymer Materials Science and Engineering Meeting, 2004, American Chemical Society, Philadelphia, PA.
18. Wang, Z.; Pinnavaia, T. J. Chem Mater 1998, 10, 3769.
19. Xiong, J.; Liu, Y.; Yang, X.; Wang, X. Polym Degrad Stab 2004, 86, 549.
20. Yao, K. J.; Song, M.; Hourston, D. J.; Luo, D. Z. Polymer 2002, 43, 1017.
21. Tien, Y. I.; Wei, K. H. J Appl Polym Sci 2002, 86, 1741.
22. Zhang, X.; Xu, R.; Wu, Z.; Zhou, C. Polym Int 2003, 52, 790.
23. Pattanayak, A.; Jana, S. C. Polymer 2005, 46, 3394.
24. Cao, X.; Lee, L. J.; Widya, T.; Macosko, C. Polymer 2005, 46, 775.
25. Tortora, M.; Gorrasi, G.; Vittoria, V.; Galli, G.; Ritrovati, S.; Chiellini, E. Polymer 2002, 43, 6147.
26. Xu, R.; Manias, E.; Snyder, A. J.; Runt, J. J Biomed Mater Res A 2003, 64, 114.
27. Osman, M. A.; Mittal, V.; Morbidelli, M.; Suter, U. W. Macromolecules 2003, 36, 9851.
28. Chen, T. K.; Tien, Y. I.; Wei, K. H. Polymer 2000, 41, 1345.
29. Chen, T. K.; Wei, K. H. Polymer 2001, 42, 3213.
30. Bolze, J.; Kim, J.; Huang, J.; Rah, S.; Youn, H. S.; Lee, B.; Shin, T. J.; Ree, M. Macromol Res 2002, 10, 2.
31. Lee, H. S.; Wang, Y. K.; Hsu, S. L. Macromolecules 1987, 20, 2089.
32. Finnigan, B.; Martin, D.; Halley, P.; Truss, R.; Campbell, K. Polymer 2004, 45, 2249.